

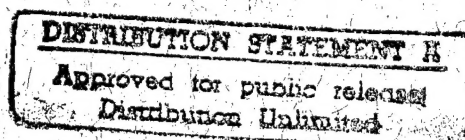
VPI-E-73-15

July 1973

# Influence of Three Dimensional Effects on the Stress Intensity Factor for Compact Tension Specimens

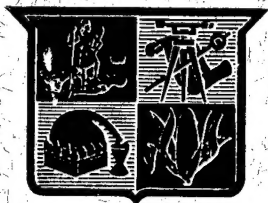
M. A. Schroedl and C. W. Smith

Department of Engineering Science and Mechanics



Prepared for:

U. S. Air Force, Air Force Systems Command  
Wright-Patterson AFB, Ohio 45433  
Contract No. 33615-72-C2111



College of Engineering,  
Virginia Polytechnic Institute  
and State University

19960328 129

61/761 194/19

Influence of Three Dimensional Effects on the Stress  
Intensity Factor for Compact Tension Specimens

M. A. Schroedl\*

and

C. W. Smith\*\*

Department of Engineering Science and Mechanics  
College of Engineering  
Virginia Polytechnic Institute and  
State University  
Blacksburg, Virginia 24061

\*Research Assistant, Department of Engineering Science and Mechanics,  
Virginia Polytechnic Institute and State University

\*\*Professor, Department of Engineering Science and Mechanics, Virginia  
Polytechnic Institute and State University

## ABSTRACT

The stress freezing technique of photoelasticity was utilized to study the stress intensity variation between full thickness and center slices of compact tension specimens for various crack lengths. Specimen geometries covered an  $a/w$  range of 0.3 to 0.7 and for values of  $w/B$  of 2 and 3.5.

Normalized SIF results for geometries within ASTM E 399-72 specifications (i.e.  $w/B = 2.0$ ,  $a/w = 0.50$ ) agreed with the ASTM solution to within experimental error. However, for  $a/w$  values outside the ASTM range (0.45 to 0.55), experimental results were measurably higher than the ASTM results for  $w/B = 2.0$  and averaged 13% higher for all  $a/w$  studied at  $w/B = 3.5$ . The center slice SIF was found to be 5 to 10% higher than the through the thickness average on all tests.

## CONTENTS

Introduction . . . . .	1
Analytical Considerations. . . . .	1
The Experiments. . . . .	3
Model manufacture . . . . .	4
Test procedure. . . . .	5
Results. . . . .	6
Discussion . . . . .	7
Summary. . . . .	8
Acknowledgements . . . . .	9
References . . . . .	10

## FIGURES

1. Local Coordinates . . . . .	13
2. Specimen Configurations . . . . .	14
3. Fringe Pattern of Full Specimen . . . . .	15
4. Local Multiplied Fringe Pattern . . . . .	16
5. Typical Set of Raw Data with Curve Fitted by TSCM . . . . .	17
6. Extrapolation from Data by TSCM to Obtain $K_{TSCM}$ . . . . .	18
7. Comparison of Results with ASTM Theory. . . . .	19
TABLE I . . . . .	20

## NOMENCLATURE

$\sigma_{ij}$	In plane stress components
$K_I$	Mode I Stress Intensity Factor (lbs/[in] <sup>3/2</sup> )
$r, \theta$	Polar coordinates (inches, radians)
$a$	Crack length (inches) (see Figure 2)
$w, B$	Specimen width (inches) (See Figure 2), Specimen thickness (Inches)
$\tau_{max}, \tau_m$	Maximum shearing stress in plane perpendicular to crack border (psi)
$K_{ap}$	Apparent stress intensity factor (lbs/[in] <sup>3/2</sup> )
$K_{TSCM}$	Approximate stress intensity factor (lbs/[in] <sup>3/2</sup> )
$n$	Fringe order
$f$	Material fringe value (#/in)
$t$	Thickness (inches)

## INTRODUCTION

A substantial effort, both from the point of view of analysis as well as fracture toughness testing, has been carried out in recent years towards the development of a universal compact plane strain fracture toughness test specimen. The analyses have taken the form of boundary collocation [1]-[5] and finite element solutions [4,5,6]. The correlation of the published results of fracture toughness testing programs is found in References [3] and [7] together with tentative test specifications and procedures. In a discussion in Reference [3], the importance of studying the three-dimensional effects photoelastically was noted. More specifically, the variation in the three-dimensional effect upon the stress intensity factor (SIF) with thickness and crack length was found to be virtually unknown. Although photoelastic stress analysis has been carried out on geometries similar to the current compact tension specimen [8], and the SIF has been estimated for the center slice [9], apparently no study has been directed towards measuring the three-dimensional effect upon the SIF directly for varying thickness and crack length. Moreover, except for the analysis of a highly idealized model [10], analytical studies have been essentially two dimensional. The present investigation was undertaken to study this effect photoelastically for a range of compact tension specimen crack lengths and thicknesses of interest to ASTM and agencies utilizing the compact tension test in order to determine the feasibility of extending the specimen geometrical ranges prescribed by ASTM E 399-72.

## ANALYTICAL CONSIDERATIONS

Photoelastic studies of crack tip stress fields have been carried out by a number of investigators [11]-[20]. One of the major difficulties in

such studies has been the problem of extracting valid SIF values from the photoelastic data. This problem has received considerable attention recently by Marloff and his associates [9], Kobayashi and his associates [21-24], and more recently by the author and his associates [25]-[29]. The author and his associates have developed two methods for extracting the SIF which have been used in a wide variety of problems. One of these methods, called the Taylor Series Correction Method (TSCM), will be employed in the present study. The philosophy and use of the method are described in the sequel.

It is well known that the elastic stresses near a crack tip in a plane normal to the crack border take a familiar singular form which may be written as:

$$\sigma_{ij} = \frac{K_I}{r^{1/2}} f_{ij}(\theta) \quad i,j = x,y \quad (1)$$

where  $K_I$  is the stress intensity factor and  $r, \theta$  are measured from the crack tip as shown in Figure 1. Since  $\sigma_{ij}$  involve singular terms, then the maximum in plane shearing stress:

$$\tau_{\max} = \frac{1}{2} \left\{ (\sigma_{yy} - \sigma_{xx})^2 + 4\tau_{xy}^2 \right\}^{1/2} \quad (2)$$

will also involve singular stresses. The authors have shown [25] that the blunted zone created by stress freezing photoelasticity near a crack tip creates a nonlinear zone very near the crack tip, but this zone is very local and light reflections from the crack tip ordinarily preclude measurements this close to the crack tip. On the other hand, there is no way to determine precisely how far away from the crack tip one can be before nonsingular terms in the stress description begin to contribute appreciably to the photoelastically measured  $\tau_{\max}$ . Since fringe loops around a crack tip tend to spread furthest along a line approximately in

a direction normal to the crack surfaces and passing through the crack tip, data are always taken along this line, reducing  $\tau_{\max}$  to the form:

$$\tau_{\max} = \tau_{\max}(r) \quad (3)$$

In order to account for boundaries other than crack surfaces themselves, TSCM expresses  $\tau_{\max}$  in the form:

$$\tau_{\max} = \frac{A}{r^{1/2}} + \sum_{N=0}^M B_N r^N \quad (4)$$

A computer program has been written to receive input data in the form of  $\tau_{\max}$ ,  $r$  from the photoelastic data, and to compute  $A$ ,  $B_N$  from the data using a least squares procedure beginning with only the first term (i.e.,  $A$ ) then  $A$ ,  $B_0$ , then  $A$ ,  $B_0$ ,  $B_1$ , etc. recomputing  $A$  each time until the  $M$ th term contributes an amount to  $\tau_{\max}$  less than the estimated experimental error. In this region, Eq. (4) is truncated and  $A = K_I/(8\pi)^{1/2}$  is determined. There is no specific truncation criterion and some judgement on the part of the investigator is required here. The convergence of the program is verified in reference [27].

For two-dimensional problems, the method corresponds to the application of the Williams Stress Function along  $\theta = \pi/2$ . Details of the program are found in Reference [27].

## THE EXPERIMENTS

A set of photoelastic experiments was designed to study the influence of crack length upon the stress intensity factor for two thicknesses and the three-dimensional effects thereof. The basic geometry of the test specimens is given in Figure 2 and the dimensions are found in Table I. The use of the  $30^\circ$  notch to simulate the crack tip stress field was sug-



gested by the result of investigations in Ref. [30] and was verified by comparing pilot test results with Wilson's boundary collocation solution. Pilot tests revealed that, due to the very low threshold value of  $K_{IC}$  for the model material above critical temperature, live loads were restricted to very small values and a counterweight was necessary in order to maintain Mode I loading on the crack tip. The force system consisting of the dead weight of the lower half of the specimen, the counterweight, and the added pin reaction served to intensify  $K_I$ . Moreover, the use of full size pins above critical temperature produced erratic results due to variations in the contact surface and frictional effects as the soft material deformed around the pins. In order to alleviate the several difficulties described above, the authors used pins which were approximately one half the hole size for the stress freezing tests and were able to obtain consistent results. Furthermore, the value of  $K_I$  was established from through the thickness room temperature fringe patterns for each test (using full size pins and much larger loads than those at stress freezing temperatures) and the thickness effect was obtained by stress freezing in a subsequent test on the same specimen. This approach implies that the auxiliary loading system consisting of the weight of the lower half of the specimen, the counterweight, and additional pin forces has no influence upon the variation in  $K_I$  through the specimen thickness. Pilot tests using only the auxiliary load system with the A-3 geometry support this assumption.

Model manufacture - All models were made from PLM-4B or Hysol 4290 stress freezing photoelastic materials by milling off 50 mils from all surfaces and maintaining ASTM tolerances throughout. All cracks were made with circular saws.

Test procedure - After inspection in the polariscope to insure stress-free specimens, the specimens were loaded at room temperature through full size pins in a dead weight system and through-the-thickness fringe photographs were obtained. Specimens were then counterweighted, hung in the oven and heated slowly to critical temperature (275°F or 300°F). After a thermal soak of about 10 hours, the live load was applied as a dead weight through the lower pin and cooling at a rate of about 2°/hr. was carried out under full load. Upon cooling, the specimen was placed in a tank of oil of the same index of refraction as the model material, and full scale and local fringe photographs were made. A full scale fringe photo through the thickness is shown in Figure 3. Next, a center slice about 0.10 in. thick was removed perpendicular to the crack border, and the fringe photography was repeated utilizing a partial mirror fringe multiplication system. All local fringe shots were made through a telescopic lens producing working prints of about 15 to 20X. A typical slice photo is shown in Figure 4.

## RESULTS

A typical set of raw fringe data from the stress freezing tests is shown in Figure 5 together with the curves fitted by TSCM. Data scatter is small and the curves fitted by TSCM fit the data well. In order to obtain a more sensitive assessment of data scatter and to illustrate how TSCM is used to obtain the SIF by extrapolation, the data of Figure 5 are replotted in Figure 6. Here the ordinate is the apparent SIF normalized with respect to the through the thickness value at the stress freezing temperature. In this case, the center slice SIF exceeded the through the thickness value by about 7%. As can be seen from Table I, for the Type A specimens with  $w/B = 2.0$ , this figure was 10% for all crack lengths between  $a/w = 0.5$  and  $0.7$ . However, for the type B specimens with  $w/B = 3.5$ , the excess of the center slice SIF over the through the thickness value varied from 5% for  $a/w = 0.5$  to 10% for  $a/w = 0.7$ . Since experimental error, on occasion, can accrue to as much as 5%, the authors do not feel that the crack length effect, noted here, is particularly significant.

A comparison of the room temperature test results with the ASTM E 399-72 equation is found in Figure 7. Because of the high sensitivity of the Type A tests to the load alignment, two test specimens were tested independently at each value of  $a/w$  in order to insure more reliable SIF values and each point on the  $w/B = 2.0$  curve represents the average of two tests. For  $w/B = 3.5$ , pilot studies showed that one test was sufficient.

Results of the study may be summarized as follows:

i) For  $w/B = 2.0$  and  $a/w = 0.50$ , experimentally determined normalized SIF values were only 2% higher than the ASTM E 399-72 values. In view of a possible 5% experimental error, this difference is judged to be negligible.

ii) Normalized SIF values over the  $a/w$  range of 0.3 to 0.7 for  $w/B = 2.0$  averaged 5% higher than the ASTM E 399-72 result and, for  $w/B = 3.5$ , averaged 13% higher than the ASTM E 399-72 result.

iii) Center slice normalized SIF values were 5 to 10% higher than through the thickness average values for both  $w/B = 2.0$  and  $w/B = 3.5$  (See Table I).

## DISCUSSION

The existing ASTM E 399-72 solution is supported by a very accurate boundary collocation solution of an idealized compact tension specimen geometry which has been verified by compliance measurements by Wilson [5] and his associates, by K calibration studies by Srawley and Brown and their associates, (unpublished) and by a recent finite element solution by Wilson and his associates [31] where he used linear strain elements in conjunction with a J Integral SIF determination. Quite recently, using a different approach, Newman [32] has used a boundary collocation solution to study effects of the pin holes for various  $a/w$  which generally agrees with the other two dimensional results.

The results cited in this study indicate that the ASTM E 399-72 result is quite accurate for  $w/B = 2.0$  and  $a/w = 0.50$ . However, when the crack lengths are varied outside the ASTM allowable range of  $a/w = 0.45$  to  $0.55$ , higher values of normalized SIF result for  $w/B = 2.0$  and still higher values result for  $w/B = 3.5$ . This suggests that if ASTM specimen geometry restrictions are to be relaxed, then additional analyses including three dimensional effects may be necessary to account for results observed here.

The above discussion is based solely upon linear elastic fracture mechanics since plasticity effects were not present in either the analytical or experimental models discussed here. In fracture toughness tests, however, plasticity is present and may exert a significant influence upon the test results if the models are not thick enough. Moreover, there is the question of the variation of constraint through the thickness in the thinner models and, in fact, whether or not plane strain predominates. Due to these complicating factors, the authors do not recommend prediction of fracture toughness results from their tests.

#### SUMMARY

A set of photoelastic experiments was conducted in order to study the influence of crack length and thickness upon the SIF for compact tension specimens within a crack length range  $a/w$  of 0.3 to 0.7 and for two thicknesses  $w/B = 2.0$  and  $w/B = 3.5$ .

The experiments confirmed the validity of the ASTM E 399-72 solution within its limits, i.e. ( $w/B = 2$ ,  $a/w = 0.45$  to  $0.55$ ) but showed measurable increases in the normalized SIF for larger values of  $a/w$  and  $w/B$ . A variation in the SIF through the specimen thickness was also identified.

The authors estimate their results to be accurate to within about 5% for linear elastic fracture mechanics comparisons. Moreover, the differences in the SIF values for the two values of  $w/B$  were only about 8%. Even though the latter difference was established from average values of some dozen or more tests in each series, the authors recommend that further tests be conducted, particularly at values of  $w/B$  of 1.0 and 6.0, in order to determine if the trends observed here extend into those ranges as well as to further substantiate the present results.

## ACKNOWLEDGEMENTS

The authors wish to acknowledge the contributions of A. E. Harms and J. J. McGowan for their laboratory and programming assistance to the project. Collocation solutions for checks were graciously supplied by W. K. Wilson. The interest and support of N. G. Tupper, Al Gunderson and D. Frederick are also appreciated. This project was sponsored by the U. S. Air Force Systems Command, Wright Field, Ohio under Contract No. 33615-72-C2111.

## REFERENCES

- [1] Wilson, W. K., "Analytical Determination of Stress Intensity Factors for the Manjoine Brittle Fracture Test Specimen", Report No. WERL-0029-3, Westinghouse Research Laboratories, August 1965.
- [2] Wilson, W. K., "Optimization of WOL Brittle Fracture Test Specimen", Report No. 66-1B4-13TLFR-R1, Westinghouse Research Laboratories, January 1966.
- [3] Brown, W. F., Jr. and Srawley, J. E., Plane Strain Crack Toughness Testing of High Strength Metallic Materials, ASTM-STP 410, pp. 14, March 1969.
- [4] Wilson, W. K., "Stress Intensity Factors for Deep Cracks in Bending and Compact Tension Specimens", J. of Engineering Fracture Mechanics, Vol. 2, No. 2, pp. 169-171, Nov. 1970.
- [5] Wilson, W. K., Tuba, I. S., and Chan, S. K., "On the Finite Element Method in Linear Fracture Mechanics", J. of Engineering Fracture Mechanics, Vol. 2, No. 1, July 1970.
- [6] Wilson, W. K., "Some Crack Tip Finite Elements for Plane Elasticity", Stress Analysis and Growth of Cracks, ASTM-STP 513, pp. 90-105, Oct. 1972.
- [7] Brown, W. F., Jr. (Editor), Review of Developments in Plane Strain Fracture Toughness Testing, ASTM-STP 463, Sept. 1970.
- [8] Leven, M. M., "Stress Distribution in the M-4 Biaxial Fracture Specimen", Research Report 65-107-STRSS R-1, Westinghouse Research Laboratories, March, 19, 1965.
- [9] Marloff, R. H., Leven, M. M., Johnson, R. L., and Ringler, T. N., "Photoelastic Determination of Stress Intensity Factors", Experimental Mechanics 11, 12, 529-539 (Dec., 1971).
- [10] Cruse, T. A. and Van Buren, W., "Three Dimensional Elastic Stress Analysis of a Fracture Specimen with an Edge Crack", International Journal of Fracture Mechanics, Vol. 7, No. 1, March 1971.
- [11] Post, D., "Photoelastic Stress Analysis for an Edge Crack in a Tensile Field", Proceedings, Society for Experimental Stress Analysis, 12, 1, pp. 99-116 (1954).
- [12] Wells, A. A. and Post, D., "The Dynamic Stress Distribution Surrounding a Running Crack - A Photoelastic Analysis", Proceedings, Society for Experimental Stress Analysis 16, 1, pp. 69-92 (1958).
- [13] Fessler, H. and Mansell, D. O., "Photoelastic Study of Stresses Near Cracks in Thick Plates", Journal of Mechanical Engineering Science 4, 3, pp. 213-225 (1962).

- [14] Kerley, B., "Photoelastic Investigation of Crack Tip Stress Distributions", GT-5 Test Report Document No. 685D 597, The General Electric Co. (March 15, 1965).
- [15] Dixon, J. R. and Strannigan, J. S., "A Photoelastic Investigation of the Stress Distribution in Uniaxially Loaded Thick Plates Containing Slits", NEL Report No. 288, National Engineering Laboratory, Glasgow, Scotland (May, 1967).
- [16] Liebowitz, H., Vanderveldt, H., and Sanford, R. J., "Stress Concentrations Due to Sharp Notches", Experimental Mechanics 7, 12, pp. 513-517 (Dec., 1967).
- [17] Smith, D. G. and Smith, C. W., "A Photoelastic Evaluation of the Influence of Closure and Other Effects upon the Local Bending Stresses in Cracked Plates", International Journal of Fracture Mechanics 6, 3, pp. 305-318 (September, 1970).
- [18] Smith, D. G. and Smith, C. W., "Influence of Precatastrophic Extension and Other Effects on Local Stresses in Cracked Plates under Bending Fields", Experimental Mechanics 11, 9, pp. 394-401 (Sept. 1971).
- [19] Smith, D. G. and Smith, C. W., "Photoelastic Determination of Mixed Mode Stress Intensity Factors", VPI-E-70-16, June 1970. J. of Engineering Fracture Mechanics 4, 2, pp. 357-366 (June 1972).
- [20] Marry, G. R. and Smith, C. W., "A Study of Local Stresses Near Surface Flaws in Bending Fields", Stress Analysis and Growth of Cracks, ASTM STP 513, pp. 22-36 (October 1972).
- [21] Bradley, W. B. and Kobayashi, A. S., "An Investigation of Propagating Cracks by Dynamic Photoelasticity", J. of Experimental Mechanics, 10, 3, pp. 106-113 (March 1970).
- [22] Bradley, W. B. and Kobayashi, A. S., "Fracture Dynamics - A Photoelastic Investigation", J. of Engineering Fracture Mechanics, 3, 3, pp. 317-332 (Oct. 1971).
- [23] Kobayashi, A. S., Wade, B. G., Bradley, W. B. and Chiu, S. T., "Crack Branching in Homalite-100 Sheets", TR-13, Dept. of Mechanical Engineering, College of Engineering, University of Washington (June 1972).
- [24] Kobayashi, A. S. and Wade, B. G., "Crack Propagation and Arrest in Impacted Plates", TR-14, Department of Mech. Engineering, College of Engineering, University of Washington (July 1972).
- [25] Schroedl, M. A., McGowan, J. J. and Smith, C. W., "An Assessment of Factors Influencing Data Obtained by the Photoelastic Stress Freezing Technique for Stress Fields Near Crack Tips", VPI-E-72, (in press) J. of Engineering Fracture Mechanics.
- [26] Schroedl, M. A., and Smith, C. W., "Local Stresses Near Deep Surface Flaws Under Cylindrical Bending Fields", (in press) Proc. of Sixth National Symposium on Fracture Mechanics (September 1972).



- [27] Schroedl, M. A., McGowan, J. J. and Smith, C. W., "Determination of Stress Intensity Factors from Photoelastic Data with Application to Surface Flaw Problems", (in press) VPI-E-73-1 Report (1973).
- [28] Harms, A. E. and Smith, C. W., "Stress Intensity Factors in Long Deep Surface Flaws in Plates Under Extensional Fields", (in press) VPI-E-73-2, Feb. 1973.
- [29] Smith, C. W., "Use of Three Dimensional Photoelasticity in Fracture Mechanics", Invited Paper, Fracture Mechanics Applications Session, Third International Congress on Experimental Mechanics, Los Angeles, Calif., May 13-18, 1973.
- [30] Gross, B. and Mendelson, A., "Plane Elasto-Static Analysis of V-Notched Plates" International Journal of Fracture Mechanics, V8, n3, pp. 267-276, September 1972.
- [31] Wilson, W.K., Chan, S.K. and Gabrielse, S.E., "Elastic Displacements for Compact Tension Specimens", Westinghouse Research Laboratories Scientific Paper No. 71-1E7-FMPWR-P5, Sept. 13, 1971.
- [32] Newman, J.C. "Stress Analysis of the Compact Specimen Including Effects of Pin Loading" Submitted to Editorial Committee of Seventh National Symposium on Fracture Mechanics.

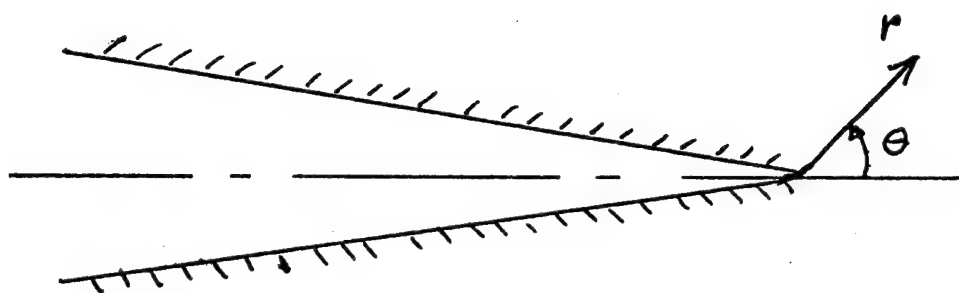


Fig. 1 Local Coordinates-

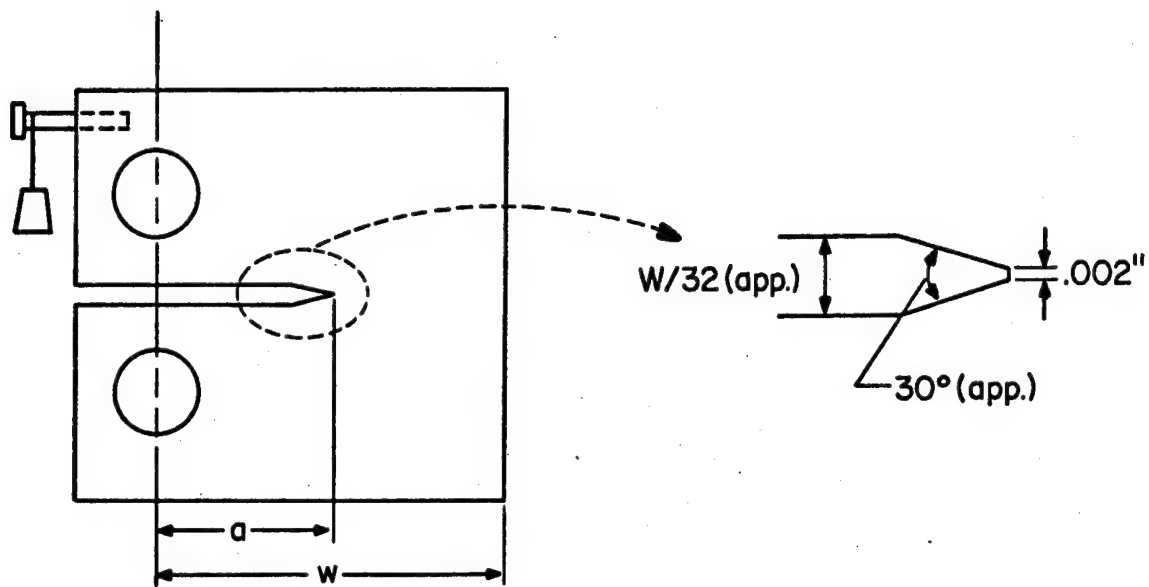


Fig. 2 Specimen Configurations

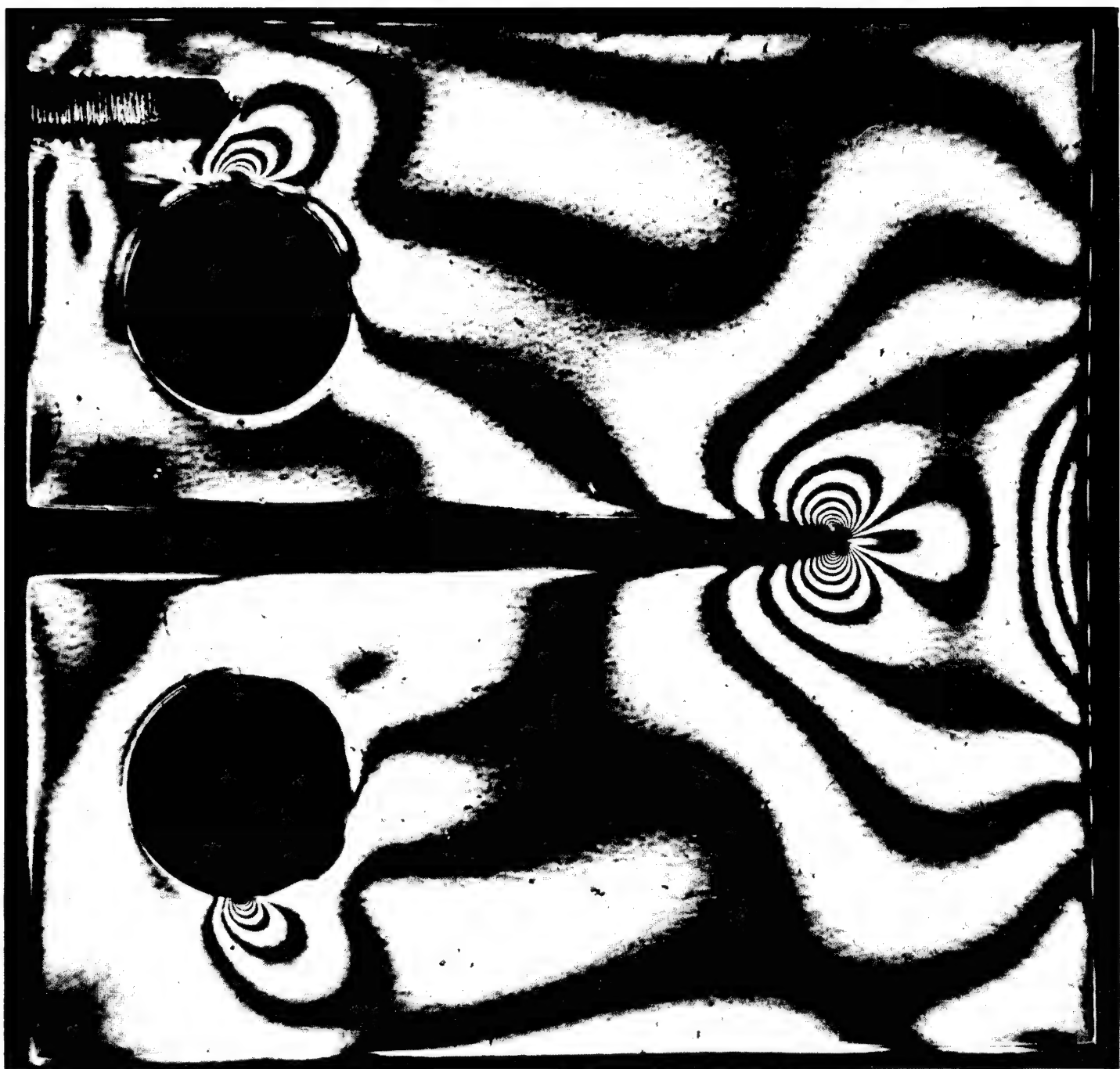


Fig. 3 Fringe Pattern of Full Specimen

COPY AVAILABLE BY THE SYSTEMS FOR THE FORTH FORTH REPRODUCTION

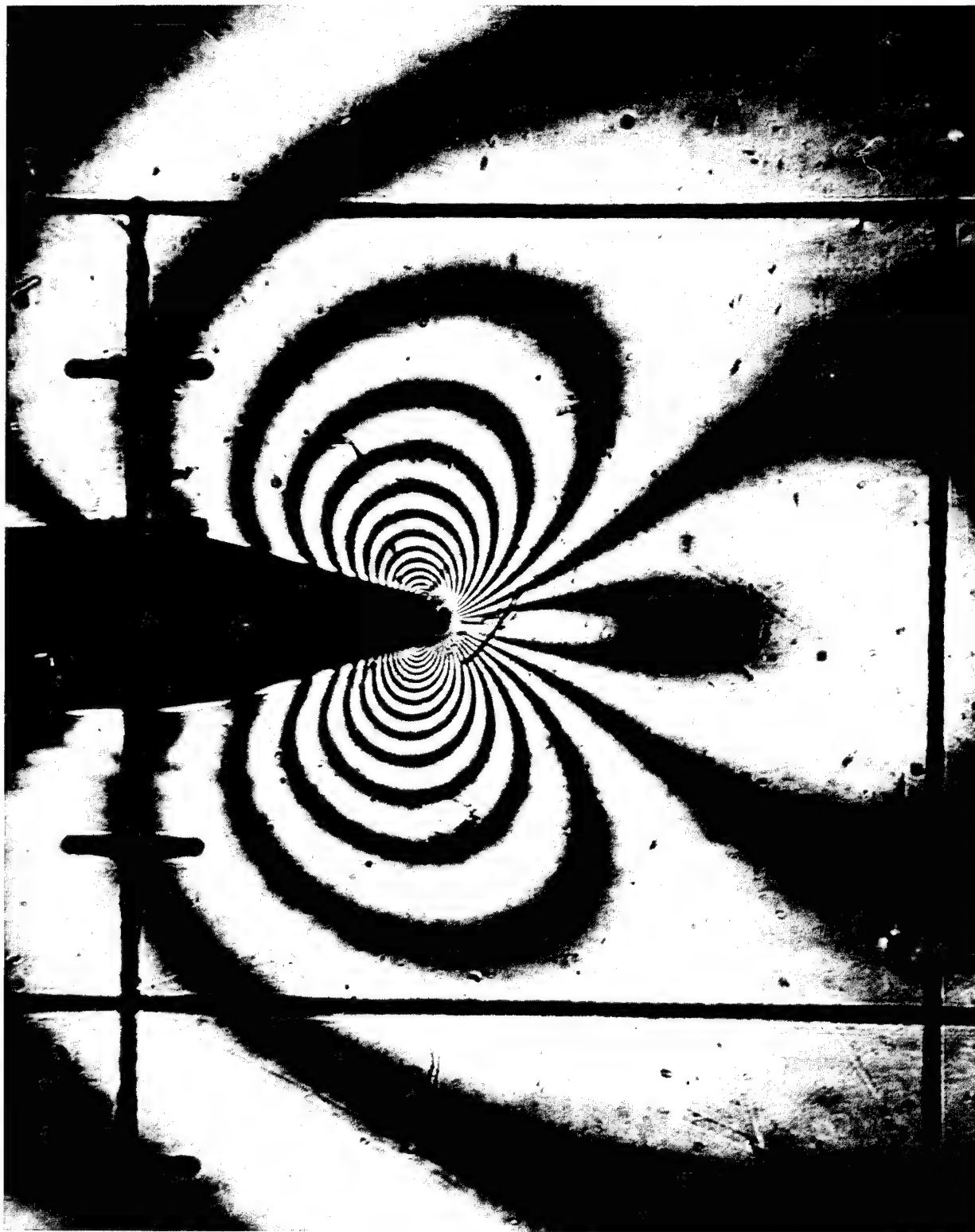


Fig. 4 Local Multiplied Fringe Pattern

COPY AVAILABLE TO DISC DOWN FROM TERRACE POINT ANCHORAGE REPRODUCTION

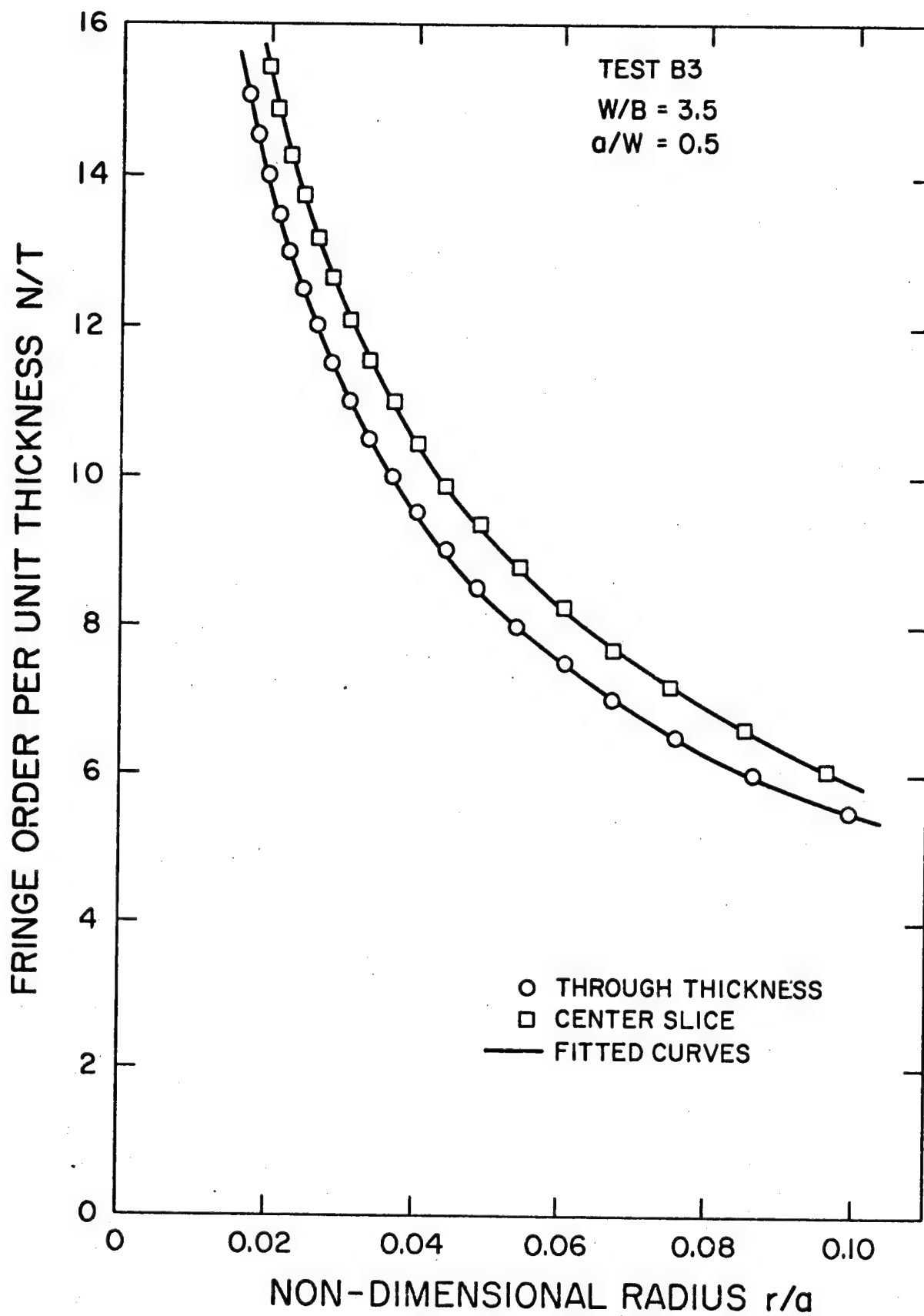


Fig. 5 Typical Set of Raw Data with Curve Fitted by TSCM

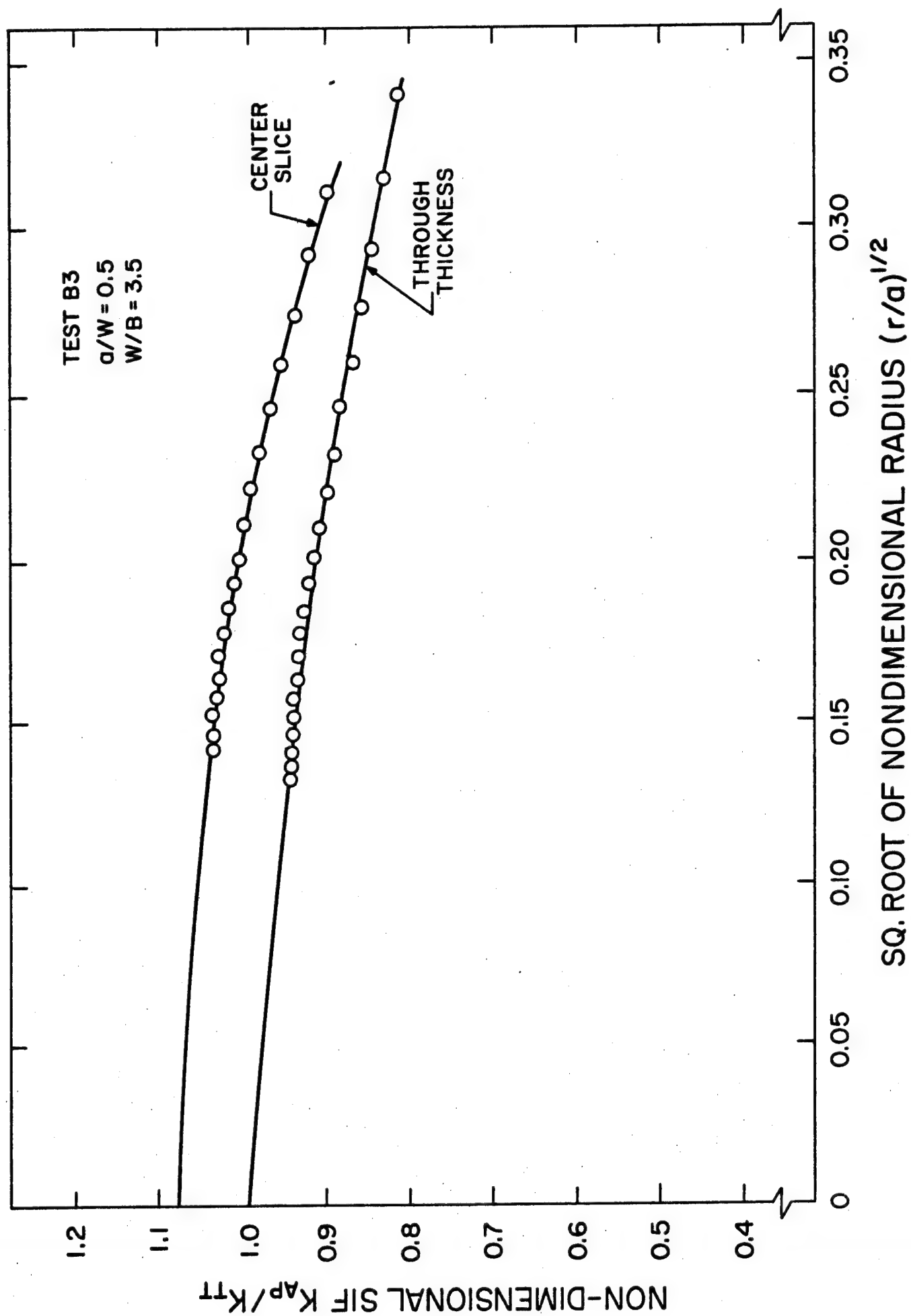


Fig. 6 Extrapolation from Data by TSCM to Obtain  $K_{TSCM}$

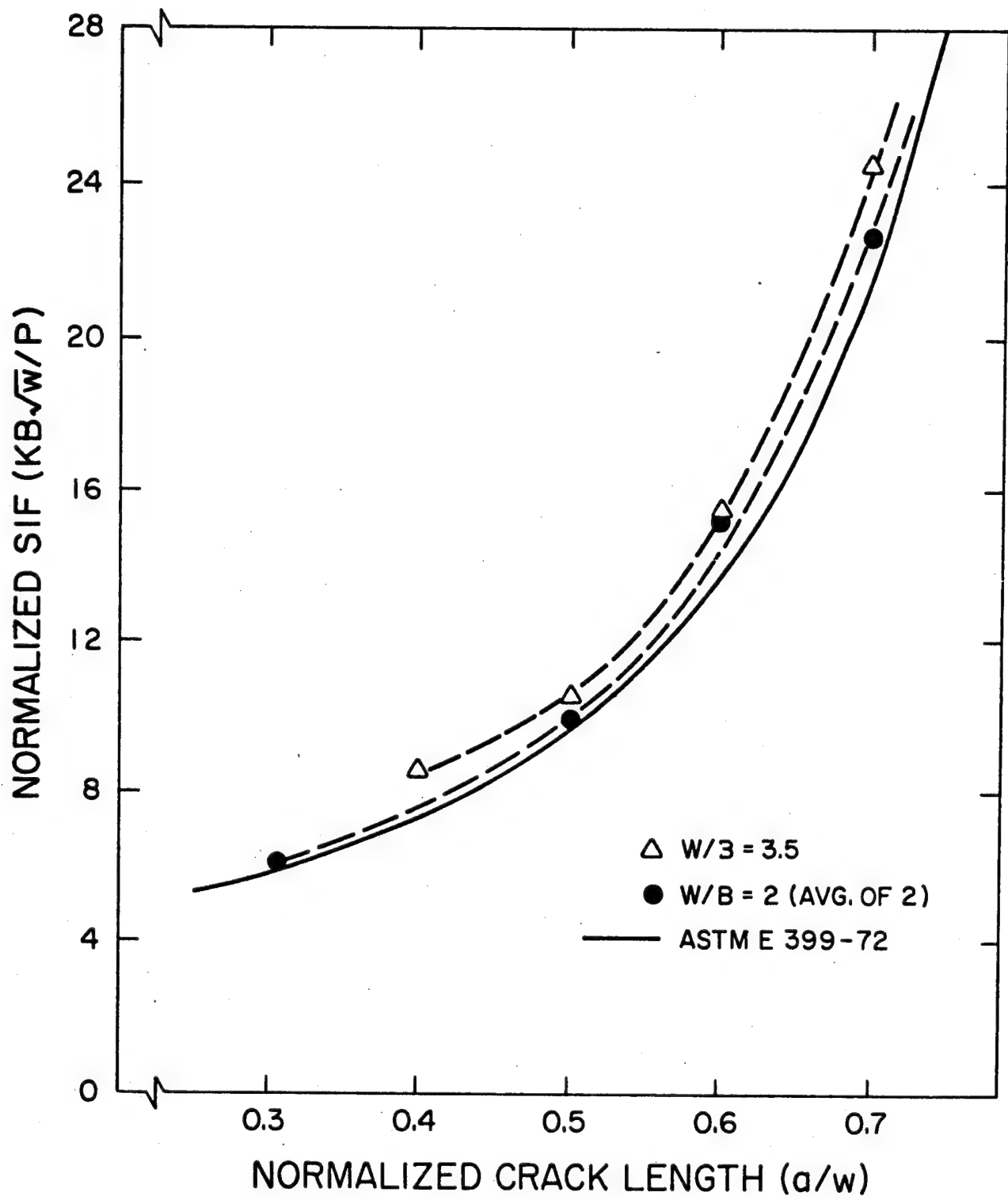


Fig. 7 Comparison of Results with ASTM Theory



TABLE I

Test	Geometry				Room Temperature Values		Stress Freezing Values
	a(in)	w(in)	B(in)	a/w	$\frac{K_{exp} B\sqrt{w}}{P}$	$\frac{K_{theo} B\sqrt{w}}{P}$	
A-1	0.525	3.50	1.750	0.30	6.0	5.9	1.08
A-2	0.875	1.75	0.875	0.50	9.7a	9.6	1.10
A-3	1.05	↓	↓	0.60	15.1a	13.5	1.10
A-4	1.23	↓	↓	0.70	22.3a	21.4	1.10 <sup>b</sup>
B-1	1.40	3.50	1.00	0.40	8.4	7.3	1.05 <sup>b</sup>
B-2	1.58	↓	↓	0.45	9.2b	8.3	1.06
B-3	1.75	↓	↓	0.50	10.5	9.6	1.07
B-4	1.93	↓	↓	0.55	12.3b	11.3	1.08 <sup>b</sup>
B-5	2.10	↓	↓	0.60	15.6	13.5	1.09
B-6	2.45	↓	↓	0.70	24.5	21.4	1.10

a = Average of two tests

b = Estimated or extrapolated from tests on similar or identical geometry

$K_{exp}$  = Experimental SIF Averaged Through Thickness at Room Temperature

$K_{theo}$  = Theoretical SIF ASTM E 399-72

$K_{cs}$  = Experimental SIF Center Slice - Stress Frozen

$K_{TT}$  = Experimental SIF Through Thickness - Stress Frozen

P = Applied Load

## DISTRIBUTION LIST

(Virginia Polytechnic Institute  
and State University)

Commanding General  
U.S. Army Natick Laboratories  
ATTN: Mr. E. W. Ross, Jr.  
Natick, Mass. 01762

Lehigh University  
ATTN: Dr. G. C. Sih  
Bethlehem, Pa. 18015

Commanding Officer  
Frankford Arsenal  
ATTN: Mr. P. D. Flynn  
Bridge & Tacony Streets  
Philadelphia, Pa. 19137

Battelle Memorial Institute  
ATTN: Dr. G. T. Hahn  
505 King Avenue  
Columbus, Ohio 43201

General Electric Company  
ATTN: A. J. Brothers, Materials and  
Processes Lab.  
Schenectady, New York 12010

United States Steel Corporation  
ATTN: Mr. S. T. Rolfe, Applied  
Research Lab.  
Monroeville, Pa. 15146

University of Illinois  
ATTN: Mr. H. T. Corten, Department of  
Theoretical & Applied Mechanics  
212 Talbot Lab.  
Urbana, Illinois 61803

Westinghouse Electric Company  
ATTN: Mr. E. T. Wessel, R&D Center  
Pittsburgh, Pa. 15200

Carnegie Institute of Technology  
ATTN: Dr. J. L. Swedlow  
Schenley Park  
Pittsburgh, Pa. 15213

Rensselaer Polytechnic Institute  
ATTN: Prof. J. C. Janz, Chairman of  
Chemistry Department  
Troy, New York 12180

Syracuse University  
ATTN: Dr. H. W. Liu  
Syracuse, New York 13210

Commanding Officer  
U.S. Army Aviation Material  
Laboratories  
ATTN: Mr. C. D. Roach  
Fort Eustis, Virginia 23604

University of California  
ATTN: W. W. Gerberich, Department of  
Mineral Technology  
Berkeley, Calif. 94700

University of Illinois  
ATTN: Prof. D. Drucker, Dean of School  
of Engineering  
Champaign, Illinois 61820

University of Washington  
ATTN: Prof. A. Kobayashi, Department  
of Mechanical Engineering  
Seattle, Washington 98105

Technical Director  
U.S. Army Materials & Mechanics  
Research Center  
ATTN: Mr. J. Bluhm  
Watertown, Mass. 02172

Brown University  
ATTN: Dr. J. R. Rice  
Providence, Rhode Island 02912

University of Connecticut  
ATTN: Dr. A. J. McEvily, Head,  
Dept. of Metallurgy U-139  
Dr. N. D. Greene, Metallurgy  
Dept.  
Storrs, Conn. 06268

No. of  
Copies

Office of the Director of Defense Research & Engineering  
ATTN: Assistant Director of Materials  
The Pentagon  
Washington, D. C. 20315

1

Commander  
Defense Documentation Center  
Cameron Station, Bldg. 5  
5010 Duke Street  
Alexandria, Virginia 22314

20

Commanding General  
U.S. Army Material Command  
ATTN: AMCRD  
AMCRD-R, Mr. H. Cohen  
AMCRD-W  
AMCRD-TC

1  
1  
1  
1

Bldg. T-7  
Washington, D. C. 20315

Commanding General  
U.S. Army Weapons Command  
ATTN: AMSWE-LCD  
AMSWE-PPR  
AMSWE-RDA  
AMSWE-RDR

1  
1  
1  
1

Rock Island, Illinois 61201

Commanding General  
U.S. Army Tank-Automotive Command  
ATTN: AMSTA-BSL  
AMSTA-BMM  
Warren, Michigan 48090

1  
1

Commanding General  
U.S. Army Munitions Command  
ATTN: AMSMU-SS-EC  
Dover, New Jersey 07801

1

Commanding Officer  
Army Research Office  
Office Chief Research & Development  
ATTN: Physical Sciences Division  
3045 Columbia Pike  
Arlington, Virginia 22207

2

Commanding Officer  
U.S. Army Research Office (Durham)  
Box CM, Duke Station  
Durham, North Carolina

6

Commanding Officer  
Rock Island Arsenal  
ATTN: SWERI-RDD  
Rock Island, Illinois 61202

Copies

Director  
Naval Research Laboratory  
Attn: Dr. J. M. Krafft, Code 8430 1  
Mr. W. S. Pellini, Code 6300 1  
Washington, D.C. 20390

Dr. G. R. Irwin  
University of Maryland  
Department of Mechanical Engineering  
College Park, Maryland 20742 1

Commander  
Wright-Patterson Air Force Base  
ATTN: AFML(MAAA)  
Hq., Aeronautical Systems Division  
Ohio 45433 5

Commander  
George C. Marshall Space Flight Center  
ATTN: M-S&M-M 1  
M-F&AEM, Bldg. 4720 1  
Huntsville, Alabama 35809

NASA Scientific and Technical Information Facility  
ATTN: Acquisitions Branch  
P. O. Box 33  
College Park, Maryland 20740 1

Mr. Robert L. Shannon, Extension Manager  
U.S. Atomic Energy Commission  
Division of Technical Information Ext.  
P. O. Box 62  
Oak Ridge, Tennessee 37831 2

Defense Metals Information Center  
Battelle Institute  
505 King Avenue  
Columbus, Ohio 43201 1

Commanding Officer  
U.S. Army Materials Research Agency  
ATTN: AMXMR-Technical Information Center  
Watertown, Mass. 02172 2

Commanding General  
Aberdeen Proving Ground  
ATTN: AMXCC - Dr. C. Pickett 1  
AMXCC - Technical Library 1  
Maryland 21003

Commanding Officer  
U.S. Army Mob Equip Research & Dev. Center  
ATTN: Technical Documents Center  
Fort Belvoir, Va. 22060 2

Commanding General  
U.S. Army Electronics Command  
Fort Monmouth, New Jersey 07703 1

Copies

Commandant  
HQ, U.S. Army Aviation School  
ATTN: Office of the Librarian  
Fort Rucker, Alabama 36362

1

Commanding Officer  
Frankford Arsenal  
Philadelphia, Pa. 19137

1

Commanding Officer  
Picatinny Arsenal  
Dover, New Jersey 07801

1

Commanding General  
Redstone Arsenal  
ATTN: Documentation & Technical Information Branch  
AMSMI-RRS  
AMSMI-RKK  
AMSMI-RSM  
Alabama 35809

2

1

1

1

Commanding Officer  
Plastics Technical Evaluation Center  
ATTN: SMUPA-VP3  
Picatinny Arsenal  
Dover, New Jersey 07801

1

Commanding Officer  
Watervliet Arsenal  
ATTN:

SWEWV-RDR Dr. M. Hussain

1

SWEWV-RDR Dr. J. H. Underwood  
SWEWV-RDR Mr. J. F. Throop

1

1

Watervliet, New York 12189

Mr. George Vrooman  
SWEWV-RDT-6  
Document Libraries  
Watervliet Arsenal  
Watervliet, New York 12189

1

Mr. Charles Eldridge  
Structures and Mechanics Laboratory  
Research and Development Director  
U. S. Army Missile Command  
Huntsville, Alabama

1

Commanding Officer  
Watervliet Arsenal  
ATTN: SWEWV-RDT-TP, Mr. John Barnewall  
Watervliet, New York 12189

6

Copies

Mr. J. G. Kaufman Alcoa Research Laboratory P. O. Box 772 Freeport Rd. New Kensington, Pa. 15068	1
Dr. T. D. Dudderar Room 1A-105 Bell Telephone Labs Mountain Avenue Murray Hill, N. J. 07971	1
Mr. W. F. Brown NASA Lewis Research Center Cleveland, Ohio 44135	1
Dr. Royce Forman NASA Manned Spacecraft Center Houston, Texas 77058	1
Dr. F. W. Smith Dept. of Mechanical Engineering Colorado State University Fort Collins, Colorado	1
Mr. N. G. Tupper AFFDL/FBA Wright-Patterson AFB, Ohio 45433	1
Materials Division Structural Integrity Branch Mail Stop 465 NASA Langley Research Center Hampton, Va. 23365 ATTN: Dr. John R. Davidson Dr. Herbert A. Leybold Dr. John Crews Mr. J. C. Newman, Jr. Dr. Wolf Elber	1 1 1 1 1 1
Mr. Howard Wood AFFDL/FBA Wright-Patterson AFB, Ohio 45433	1
Mr. Al Gunderson AFFDL/FBA Wright-Patterson AFB, Ohio 45433	1

Unclassified

Security Classification

## DOCUMENT CONTROL DATA - R &amp; D

(Security classification of title, body of abstract and indexing annotation must be entered when the overall report is classified)

## 1. ORIGINATING ACTIVITY (Corporate author)

Virginia Polytechnic Institute and State University

## 2a. REPORT SECURITY CLASSIFICATION

Unclassified

## 2b. GROUP

## 3. REPORT TITLE

Influence of Three Dimensional Effects on the Stress Intensity Factor for Compact Tension Specimens

## 4. DESCRIPTIVE NOTES (Type of report and inclusive dates)

## 5. AUTHOR(S) (First name, middle initial, last name)

M.A. Schroedl and C.W. Smith

## 6. REPORT DATE

April 1973

## 7a. TOTAL NO. OF PAGES

20

## 7b. NO. OF REFS

32

## 8a. CONTRACT OR GRANT NO.

No. 33615-72-C2111

## b. PROJECT NO.

## 9a. ORIGINATOR'S REPORT NUMBER(S)

## c.

## 9b. OTHER REPORT NO(S) (Any other numbers that may be assigned this report)

## d.

## 10. DISTRIBUTION STATEMENT

Approved for public release; distribution unlimited.

## 11. SUPPLEMENTARY NOTES

## 12. SPONSORING MILITARY ACTIVITY

Air Force Systems Command  
United States Air Force  
Wright-Patterson AFB, Ohio 45433

## 13. ABSTRACT

The stress freezing technique of photoelasticity was utilized to study the stress intensity variation between full thickness and center slices of compact tension specimens for various crack lengths. Specimen geometries covered an a/w range of 0.3 to 0.7 and for values of w/B of 2 and 3.5.

Normalized SIF results for geometries within ASTM E 399-72 specifications (i.e. w/B = 2.0, a/w = 0.50) agreed with the ASTM solution to within experimental error. However, for a/w values outside the ASTM range (0.45 to 0.55), experimental results were measurably higher than the ASTM results for w/B = 2.0 and averaged 13% higher for all a/w studied at w/B = 3.5. The center slice SIF was found to be 5 to 10% higher than the through the thickness average on all tests.

DD FORM 1473  
1 NOV 66REPLACES DD FORM 1473, 1 JAN 64, WHICH IS  
OBSOLETE FOR ARMY USE.

Unclassified

Security Classification

Unclassified

Security Classification

14. KEY WORDS	LINK A		LINK B		LINK C	
	ROLE	WT	ROLE	WT	ROLE	WT
Stress Intensity Factor Compact Tension Specimen Photoelasticity Crack Tip Stress Fields						

Unclassified

Security Classification